Ecology, 95(10), 2014, pp. 2815–2825
© 2014 by the Ecological Society of America

Empirical tests of within- and across-species energetics in a diverse plant community

Erica A. Newman,[1,2,6] Mary Ellen Harte,[3] Natalie Lowell,[2,4] Mark Wilber,[2,5] and John Harte[1,2]

[1]*Energy and Resources Group, University of California, 310 Barrows Hall, Berkeley, California 94720 USA*
[2]*Department of Environmental Science, Policy, and Management, University of California, 130 Mulford Hall, Berkeley, California 94720 USA*
[3]*Rocky Mountain Biological Laboratory, Gothic, Colorado 81224 USA*
[4]*School of Marine and Environmental Affairs, University of Washington, 3707 Brooklyn Avenue Northeast, Seattle, Washington 98105 USA*
[5]*Department of Ecology, Evolution and Marine Biology, University of California, 2111 Noble Hall, Santa Barbara, California 93106 USA*

Abstract. Many fundamental properties of ecological systems and interactions are tied to body size and a related metric, the metabolic rate distribution, both within and across species. A previously proposed maximum entropy theory of ecology (METE) predicts numerous interrelated macroecological patterns, including spatial distributions of individuals within species, abundance distributions across species, species area relationships, and distributions of metabolic rates of all individuals within a community. Extensive tests of METE's macroecological predictions generally support the theory, but two related predictions have not been evaluated against full community census data: the distribution of metabolic rates of individuals within species as a function of the abundance of the species and the distribution of average individual metabolic rates across species. We test the metabolic predictions of METE for herbaceous plants in a subalpine meadow and show that while this theory realistically predicts the distribution of individual metabolic rates across the entire community, the within- and across-species predictions generally fail. We also test the energy-equivalence type prediction that arises as a consequence of the prediction for the distribution of average individual metabolic rates across species. We suggest several possible explanations for the empirical deviations from theory, and distinguish between the expected deviations caused by ecological disturbance and those deviations that might be corrected within the theory.

Key words: energy equivalence; information entropy; macroecology; maximum entropy theory of ecology, METE; metabolism; scaling laws.

Introduction

Many fundamental properties of ecosystems are tied to body sizes of their component members, both at the individual and species level. Within a species, body size often correlates to fitness and metabolism, whereas, considering all species in a community, body size will correlate to metabolism, abundance, trophic activity, ecological and life history traits, and community stability. The distribution of body sizes within a community is potentially important for understanding community properties and function, as well as predicting conservation implications of invasive species or changes that will result following species extirpation in a community. Accordingly, body-size distributions have attracted much theoretical and empirical attention (Damuth 1981, 1987, Niklas and Enquist 2001, Brown et al. 2004, Muller-Landau et al. 2006, White et al. 2007, Clauset et al. 2009, Mori et al. 2010, Harte 2011). Macroecologists have attempted to connect body size to abundances of species using power-law models and experimental observations, but despite these efforts, there had not been an overarching theoretical framework for connecting metrics that describe abundance and metabolics until the development of the maximum entropy theory of ecology (METE; Harte et al. 2008, 2009, Harte 2011).

METE is an extremely general macroecological theory that predicts spatial, abundance, and metabolic rate distributions of species, and the interrelationships of these metrics for any system defined by a set of basic community state variables. It, therefore, also predicts body-size distributions if a metabolic-scaling relationship between metabolism and body size is assumed. Unlike other unified theories of ecology and diversity (Hubbell 2001, de Aguiar et al. 2009, McGill 2010), METE uses no adjustable parameters and is instead formulated using the procedure of maximizing information entropy, a technique that has been proven to yield least-biased probability distributions that are consistent with prior knowledge in the form of constraints on those distributions (Jaynes 1979, 1982, 2003). Constraints may take the form of the empirical ranges, means, or higher

Manuscript received 21 October 2013; revised 3 April 2014; accepted 4 April 2014. Corresponding Editor: N. J. B. Kraft.
[6] E-mail: newmane@berkeley.edu

moments of values of one or more independent variables of a system, or outcomes of system measurements (Harte et al. 2008; Harte and Newman 2014).

As inputs, METE uses four measured state variables: S_0, the total number of species; N_0, the total number of individuals; E_0, the total metabolic rate of all individuals; and A_0, an arbitrary but specified spatial scale. Mathematical forms of macroecological metrics are derived from constraints arising from ratios of the four state variables. Various empirical tests of species–area relationships (SARs), endemics–area relationships (EARs), and species-abundance distributions (SADs) indicate support for theoretical predictions of those metrics (Harte et al. 2008, 2009, White et al. 2012), but the metabolic predictions of METE require more empirical validation, including tests of the predicted within-species distribution of metabolic rates and the predicted distribution of species' average metabolic rates across all species (see Xiao et al. 2013). Using the diverse subalpine plant community of the Rocky Mountains (see Plate 1), we investigate the extent to which METE makes realistic predictions about the metabolic rate distributions, both within and across species.

Methods

Site description

Sampling was carried out in the summer of 2012 in Gunnison National Forest, Gunnison County Colorado, USA at a site located 6.8 km (4.2 miles) north of the Gothic town site (plot location 39°0′20.29″ N, 107°1′54.67″ W) at an elevation of 3189 m. The study plot was sited in an area that minimized the extent of disturbance in the forms of Northern pocket gopher (*Thomomys talpoides*) mounds and anthropogenic disturbance including cattle grazing, human presence, and invasive grasses and forbs. We chose a site that received constant moisture from a nearby creek to offset effects of the drought occurring in 2012, but overall disturbance level was still moderate. The dominant trees of this area are primarily Engelmann spruce (*Picea engelmannii*) and Subalpine fir (*Abies bifolia*) in stands surrounding but distinct from the meadow communities. Open meadows contain shrubby *Potentilla fruticosa* and large patches of the herbaceous *Veratrum californicum*, while moister areas of the meadow have large patches of mixed-species shrubby willows (dominated by *Salix planifolia*).

Sampling

A 4 × 4 m plot was gridded into 1-m cells. Plants were censused and recorded with both a cell number and an x and y spatial coordinate reference within the cell for ease of relocating individual plants. After locating all individuals, we assigned each a unique identification and counted all living leaves. We clipped a representative fraction of the living aboveground biomass at ground level from each plant for analysis (Cornelissen et al. 2003). We collected 20–50% of the live biomass of large plants and collected small plants whole (see Appendix A for more detail). We placed samples into plastic bags and transported them to a lab in a cooler with ice to prevent leaf area shrinkage (following the methods of Blonder et al. 2012), where they were rehydrated and placed on a flatbed scanner. We analyzed and recorded leaf and stem area separately for each sample using the software ImageJ 1.46 (Abramoff et al. 2004). We calculated total photosynthetic area of an individual plant by applying mean area per leaf sampled from that plant to its total leaf count and adding its total stem area. This was done on an individual basis in order to take into account all plants' life stages and leaf size variation. Because only living material was included in this study, we excluded plants with all leaves senesced at the time of sampling, which excluded some individual plants and may have excluded one or more early blooming species altogether. Similarly, we excluded immature plants that measured less than 1 cm in height and breadth at the time of sampling.

Metabolic calculations

Allometric work by Niklas and Enquist (2001) has established that leaf area (A_L) scales as body mass (M) to the three-fourths power ($A_L \propto M^{3/4}$) across species. Subsequent studies confirm this relationship between simple metrics of leaf area (or photosynthetic area, including green stems), leaf mass, body mass, and metabolic rates (Reich et al. 2006, Deng et al. 2008, Makarieva et al. 2008). Metabolic scaling theory states that $B \propto M^{3/4}$, where B is metabolic rate (Niklas and Enquist 2001). By this logic, it follows that $A_L \propto B$; that is, the relationship between leaf area and metabolic rate is approximately linear. Although the metabolic rate should in fact represent the instantaneous metabolism of each plant, simultaneous measurements of whole-plant photosynthetic processes were infeasible. A measure of total photosynthetic area, which is the result of the energy an individual has accrued over time (time integrated energy), is therefore suitable as a proxy of the time-averaged metabolic rate. Similar justification in other macroecological studies allows the estimation of metabolism from diameter at breast height (dbh) with scaling assumptions (see for example Muller-Landau et al. 2006, Rüger and Condit 2012, Xiao et al. 2013) and by organisms' mass (Glazier 2006).

Using the proportional relationship between total leaf area and total metabolic energy of a plant $A_L \propto B$, we can then estimate the METE state variable energy (E_0) and the metabolic rate of an individual, ε, by units of normalized photosynthetic area for the herbaceous plants considered here. E_0 is related to ε by the relationship $E_0 = \sum_{i=1}^{N_0} \varepsilon_i$, with the continuous variables ε and E_0 normalized through a linear transformation such that the individual with the lowest metabolic rate has $\varepsilon = 1$ (that is, $\varepsilon_i = a_i/\min(a_i)$, where a_i is photosynthetic area for individual i and $\min(a_i)$ is the total photosynthetic area of the smallest individual in the community). We note that the quantity historically referred to in the metabolic

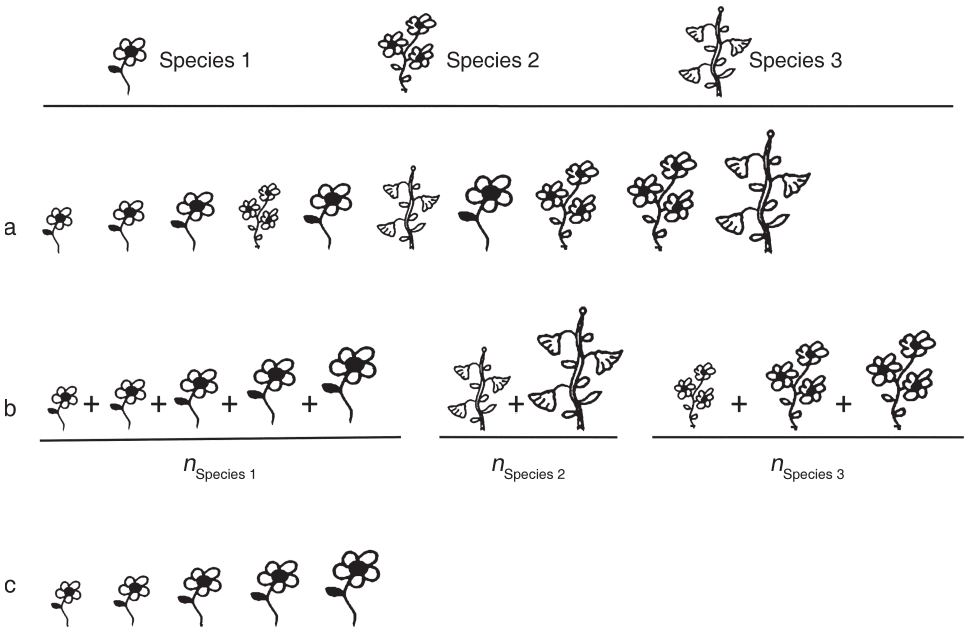

FIG. 1. Visual representation of what is modeled by (a) the individual-level energy distribution (IED), (b) the distribution of average metabolic rates across species or average species energy distribution (ASED), and (c) one example of the distribution of metabolic rates across the individuals in a single species of abundance n, also known as the species-level energy distribution (SED). Differences in sizes of icons correspond to differences in organisms' sizes and metabolic rates.

literature as either energy, metabolic energy, or respiratory metabolic rate actually has physical units of power. We choose to use the term "metabolic rate distribution" and note that all energy labels and metrics of energy are actually in units of power.

We test three metrics predicted by METE for the subalpine plant community: the distribution of metabolic rates of all individuals in a community, the distribution of average individual metabolic rates across species (both of these being community-level metrics), and the distribution of metabolic rates of individuals within species as a function of the abundance of the species (a species-level metric). See Fig. 1.

Individual-level energy distribution

The individual-level energy distribution (IED) describes the distribution of metabolic rates over all of the individuals in the community and is represented by $\Psi(\varepsilon)$

$$\Psi(\varepsilon \,|\, S_0, N_0, E_0) = \lambda_2 \times \beta \frac{e^{-\gamma}}{(1 - e^{-\gamma})^2} \tag{1}$$

where ε is the metabolic rate of an individual, $\gamma = \lambda_1 + \lambda_2\varepsilon$; λ_1 and λ_2 are the Lagrange multipliers given by $\lambda_1 = \beta - \lambda_2$ and $\lambda_2 = S_0/(E_0 - N_0)$, respectively; and β satisfies the approximate relationship $\beta[\ln(1/\beta)] \approx S_0/N_0$ (Harte et al. 2008, 2009). A derivation of this expression and discussion of simplifying assumptions is available in Harte 2011, where a more exact expression for β is given. $\Psi(\varepsilon)$ is a continuous distribution on the domain of 1 to E_0. The integral of $\Psi(\varepsilon)$ from 1 to E_0 is 1, and so $\Psi(\varepsilon)$ is the normalized probability density function for metabolic rates of all individuals in the community.

Average species energy distribution

The average species energy distribution (ASED) is the distribution, across all the species in the community, of metabolic rates averaged over individuals within species and is represented by $\nu(\bar{\varepsilon})$. The predicted form of the ASED of a community is

$$\nu(\bar{\varepsilon} \,|\, S_0, N_0, E_0) = \frac{1}{\ln\left(\dfrac{S_0}{\beta}\right)} \times \frac{e^{\frac{-\beta}{\lambda_2(\bar{\varepsilon}-1)}}}{(\bar{\varepsilon} - 1)} \tag{2}$$

where $(\bar{\varepsilon})$ is the average metabolic rate of the individuals for the species under consideration and is defined on the continuous domain from 0 to N_0 (Harte et al. 2008, 2009). This exact expression replaces the approximate expression in Harte (2011: Eq. 7.46) because the simplification used in Harte (2011), $\ln(1/\beta) \gg \ln(S_0)$, or equivalently $\beta \times S_0 \ll 1$, does not hold for our data. Here, the term $\ln(S_0/\beta) = \ln(1/\beta) + \ln(S_0)$ replaces $\ln(1/\beta)$.

A key relationship for understanding the ASED is the inverse relationship between the expected energy, $\bar{\varepsilon}$ for a species and its abundance n (Harte et al. 2008, Harte 2011: chapter 7)

$$\bar{\varepsilon} \approx 1 + \frac{1}{n\lambda_2}. \tag{3}$$

Although $\bar{\varepsilon}$ is not exactly inversely proportional to n, it is the case for those species for which $n \ll 1/\lambda_2$, and therefore $1/(n \times \lambda_2) \gg 1$. For our study system, the

TABLE 1. Species names, abundances, rank, and leaf-area measurements of 31 species of plants in a subalpine plot.

Code	Species	Common name	Rank in plot by n	n	Minimum metabolic rate	Maximum metabolic rate	Average metabolic rate
BOEDRU	*Boechera stricta* (syn. *Boechera drumondii*)	Tower mustard	1	103	4.694	191.013	33.970
HELQUI	*Helianthella quinquenervis*	Five nerve heliantella	2	94	77.013	38 251.850	4 680.185
VIONUT	*Crocion nuttallii* (syn. *Viola nuttallii*)	Yellow montaine violet	3	93	1.000	1 224.081	227.330
LUPARG	*Lupinus argenteus*	Silvery lupine	4	85	6.734	28 164.320	736.251
ANDSEP	*Androsace septentrionalis*	Northern rock jasmine	5	62	1.134	35.431	8.193
HYMHOO	*Hymenoxys hoopesyii*	Sneezeweed	6	55	32.363	5 719.091	956.284
FRAVES	*Fragaria vesca*	Alpine strawberry	7	54	15.119	1 223.867	207.540
POTGRA	*Potentilla gracilis* var. *nuttallii* (syn. *Potentilla gracilis*)	Slender cinquefoil	8	47	8.443	4 171.999	728.910
LIGPOR	*Ligusticum porteri* (syn. *Ligusticum porteri* var. *brevilobum*)	Osha	9	38	3.424	21 632.616	3 171.588
VICAME	*Vicia americana*	American vetch	10	33	6.248	582.964	128.913
IPOAGG	*Ipomopsis aggregata*	Scarlet gilia	11	23	7.075	467.952	72.744
THLMON	*Thlaspi montanum* (syn. *Noccaea montana*)	Candytuft, Alpine pennycress	12	20	5.821	1 494.010	118.013
SENCRA	*Senecio crassulus*	Thick-leaved groundsel	13	19	8.018	1 115.985	262.590
DELBAR	*Delphinium barbeyi*	Tall larkspur	14	16	73.235	17 051.759	2 243.050
ERIFOR	*Erigeron formosissimus*	Beautiful fleabane	15	14	14.089	14 552.655	1 578.719
LATLEU	*Lathyrus leucanthus* (syn. *Lathyrus lanzwertii* var. *leucanthus*)	Peavine, Rocky Mountain sweetpea	16	13	63.034	1 857.990	564.596
SOLMUL	*Solidago multiradiata*	Goldenrod	17	12	7.449	408.856	109.939
POLDOU	*Polygonum douglasii*	Douglas's knotweed	18	12	5.862	157.921	35.843
ERIELA	*Erigeron elatior*	Pink-headed fleabane	19	11	15.921	1 443.983	477.113
AGOGLA	*Agoseris glauca*	Mountain dandelion	20	11	20.513	714.540	192.236
DRASPE	*Draba spectabilis*	Showy draba	21	10	27.369	159.939	73.597
CASSUL	*Castilleja sulphurea*	Sulphur paintbrush	22	10	12.864	1 805.139	537.313
EUCENG	*Eucephalus engelmannii* (syn. *Aster engelmannii*)	Englemann's aster	23	8	70.823	1 589.375	607.619
ERISPE	*Erigeron speciosus*	Showy fleabane	24	8	65.799	1 415.119	573.524
SENAMP	*Senecio amplectens* (syn. *Ligularia holmii*)	Showy alpine ragwort	25	7	39.841	1 108.729	282.468
GERRIC	*Geranium richardsonii*	White geranium	26	7	21.889	1 043.685	438.361
CASSOC	*Castilleja occidentalis*	Tundra Paintbrush	27	5	69.661	310.800	226.134
VIGMUL	*Heliomeris multiflora* (syn. *Viguiera multiflora*)	Showy goldeneye	28	2	294.612	458.466	376.539
OSMOCC	*Washingtonia occidentalis* (syn. *Osmorhiza occidentalis*)	Sweet cicely	29	2	4972.977	32 451.402	18 712.189
AQUCOE	*Aquilegia flavescens* (syn. *Aquilegia coerulea*)	Colorado columbine	30	2	24.894	23 956.678	11 990.786
TAROFF	*Taraxacum officinale*†	Common dandelion	31	1	9.537	9.537	9.537

Note: All metabolic rates are in normalized units of leaf area, and n is the measured abundance of each species.
† Indicates an exotic species.

inequality holds for all species, and so the added 1 can be neglected.

Using this relationship between $\bar{\varepsilon}$ and n, we derive a probability distribution for $\bar{\varepsilon}$ from the species-abundance distribution. This probability distribution is the ASED itself (see Harte 2011:155). As a result of the functional form of Eq. 3, the smallest values of average energy per individual in a species are expected for the most abundant species, and conversely, the largest values of average energy per individual within a species are expected for species with the lowest abundances.

Because the SAD is a continuous function of a discrete variable (n), the constructed ASED distribution reflects this discrete component. The predicted ASED is only defined for values of $\bar{\varepsilon} = (1 + (1/(n \times \lambda_2))$, where n (the number of individuals of a species) is in the range $[1, N]$ (and where $N = n_{\max}$); however, empirical values of $\bar{\varepsilon}$ can take on any continuously defined value between 1 and E_0. This leads to artificial effects described in Appendix F.

Species-level energy distribution

The species-level energy distribution (SED) is the distribution of metabolic rates across the individuals in a single species of abundance n. The SED is represented by $\Theta(\varepsilon \mid n)$ and is derived from the SAD, represented by $\Phi(n)$ (from Harte 2011)

$$\Theta(n \mid \varepsilon) = \frac{R(n, \varepsilon)}{\Phi(n)} \tag{4}$$

where $R(n, \varepsilon)$ is the ecosystem structure function, a joint probability that a chosen species will have the abun-

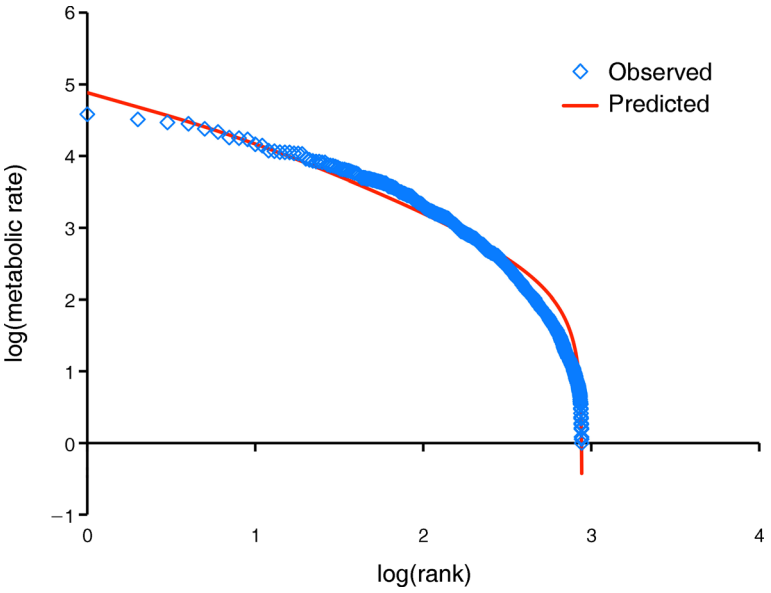

FIG. 2. Comparison of empirical data to maximum entropy theory of ecology (METE) individual-level energy distribution (IED) predictions for a subalpine plant community. This graph shows empirical and predicted IED values on a log(rank) vs. log(metabolic rate) graph for all individuals in the plot.

dance n and that a given individual picked from that species will have a metabolic rate equal to that of the smallest individual (Harte 2011). The form of the ecosystem structure function is uniquely predicted by METE when the numerical values of the state variables are known. The approximation below is the form of the function used to predict SEDs by species (Harte 2011: chapter 7)

$$\Theta(\varepsilon \,|\, n, S_0, N_0, E_0) \approx \lambda_2 n e^{-\lambda_2 n(\varepsilon - 1)} \tag{5}$$

Summing $\Theta(\varepsilon \,|\, n) \times \varepsilon$ over all possible values of ε recovers Eq. 3. Predictions of SEDs by species incorporate the overall constraint that the smallest, lowest-energy individual in the entire study system must equal the actual value normalized to $\varepsilon = 1$. The SED metric is related to the ASED, in that the predicted distribution of the means of the SEDs is the ASED.

Letting r denote rank, the rank-metabolism relationships are derived from the SED and IED, assigning the rank of $r = 1$ for the individual with the largest metabolic rate. A maximum rank of $r = n$ (by species) for the SEDs and $r = N_0$ for the IED is assigned to the individual with the lowest metabolic rate. Ranked metabolic distributions for the SED and IED are given by the following equations, respectively (Harte 2011: chapter 7)

$$\varepsilon_\theta(r, n) = 1 + (\lambda_2 n)^{-1} \times \ln\left(\frac{1}{\frac{(r - \frac{1}{2})}{n} + e^{-\lambda_2 n \times \varepsilon_{\max}}}\right) \tag{6}$$

$$\varepsilon_\Psi(r) = \frac{1}{\lambda_2} \times \ln\left(\frac{\beta N_0 + r - \frac{1}{2}}{r - \frac{1}{2}}\right) - \frac{\lambda_1}{\lambda_2} \tag{7}$$

where $\varepsilon_{\max}$ is the individual in that species with the maximum metabolic rate (largest photosynthetic area) individual. To calculate $\varepsilon_{\max}$, Eq. 7 is calculated with $r = 1$, yielding

$$\varepsilon_{\Psi,\max} = \varepsilon_\Psi(r = 1) \approx \frac{1}{\lambda_2} \log(2\beta N_0) \tag{8}$$

(Harte 2011). This equation refers to the entire individuals pool for the IED, but can be easily modified for the SEDs, so that for the SEDs, $\varepsilon_{\max} = \log(2n/n)$. The rank-metabolism predictions for the SED is modified from Harte (2011) not to contain simplifying assumptions as described for Eq. 2.

Analysis

Many analyses and calculations of differential equations for the metrics considered in this paper were carried out with Python (van Rossum and Drake 2001) in the open-source project Macroeco (*available online*)[7]. Analyses were carried out with ASED, IED, and SED metabolic-analysis scripts in the beta version of this software. Predictions from Eqs. 2, 6, and 7 were compared to the measured metabolic rate and rank-metabolism data using slope and R^2 values on log(observed) vs. log(predicted value) graphs, and

[7] http://github.com/jkitzes/macroeco

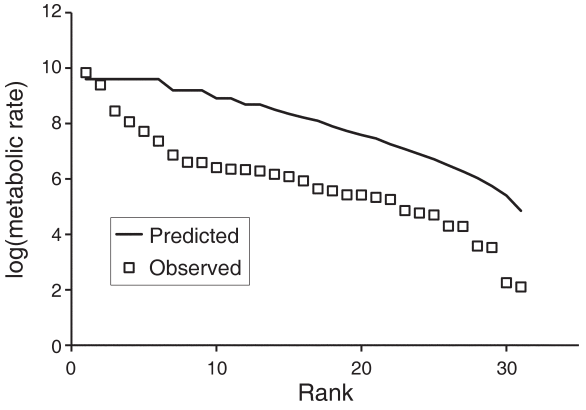

FIG. 3. ASED predictions and empirical data for a subalpine plant community where species are ranked by average metabolic rate on a rank-log(metabolic rate) plot.

Kolmogorov–Smirnov tests are performed to determine the quality of METE predictions in the subalpine plot.

RESULTS

A total of 877 plants comprising 31 species are included in this study. A complete species list for the plot and species' abundances are shown in Table 1. Calculated values for the Lagrange multipliers are $\lambda_1 = 7.0463 \times 10^{-3}$ and $\lambda_2 = 3.3806 \times 10^{-5}$ for $N_0 = 877$, $S_0 = 31$, and $E_0 = 917\,871.975$ and the parameter $\beta = 7.0801 \times 10^{-3}$. The range of total photosynthetic areas for individuals (a surrogate for body sizes) represented by our study system is greater than 38 200:1, that is, a four-orders-of-magnitude range (comparable to the ranges represented by the trees of the Smithsonian data sets, which are often used to test macroecological theory). Minimum photosynthetic area for an individual plant is $a_{\min} = 0.2793$ cm^2. Graphs of the species- and community-level energy metrics are shown in Fig. 2, IED; Fig. 3, ASED; and Fig. 4, SEDs of the 12 most abundant species. SED results for all species with $n \geq 5$ are available in Appendix B, with a summary of derived values in Appendix C, and results of the 15 most abundant species in order by average metabolic rate of an individual within a species are shown in Appendix D. Goodness of fit tests, including Kolmogorov-Smirnov (K-S) tests, are presented for all metrics in Appendix G.

Individual-level energy distribution

The METE prediction of the IED, the metabolic rate distribution for all individuals in a community, shows fairly good agreement with empirical data as a smooth, monotonically decreasing function of ranked metabolic rate, with increasingly negative slope (Fig. 2). Because the normalization of the IED requires the total predicted metabolic rate to equal the total metabolic rate of the empirical data, the curves necessarily intersect on this graph.

To test similarity between empirical and predicted curves of the IED, we construct a graph of log(observed) vs. log(predicted value) and note that a slope of nearly 1 and a high R^2 value (slope = 0.8362; $R^2 = 0.9742$) indicates that the IED performs well in predicting the metabolic rate distribution for all individuals in the community. However, a K-S test performed on 1000 bootstrapped samples does not support the null hypothesis that the observed and theoretical distributions are the same ($D = 0.1653$, where D is the Kolmogorov-Smirnov statistic for a specified cumulative distribution function; $P < 0.0001$). But, whereas the K-S test may be more appropriate because it is less sensitive to normality of a distribution than some other goodness-of-fit metrics (like Shapiro-Wilk and Anderson-Darling), it tends to reject the null hypothesis at a high rate based on deviant values and has been criticized for producing misleading results (Babu and Feigelson 2006).

Average species energy distribution

The distribution of average metabolic rates across species, the ASED, is predicted to have increasingly negative slope as a function of ranked energy if $\ln(\bar{\varepsilon})$ is plotted against rank, r, from largest average metabolic rate per species to smallest. Empirical data deviates from this pattern strongly, showing an inflected shape (Fig.3). A K-S test does not support the null hypothesis of no difference between observed and theoretical distributions ($D = 0.5484$, $P < 0.0001$, 1000 bootstrapped samples). Appendix H contains the predicted probability distribution for the ASED (ν) and additional tests of goodness-of-fit. A notable feature of the ASED is that the empirical and predicted distributions do not have the same mean.

Species-level energy distributions

The METE-predicted distributions of metabolic rates across all individuals in a single species of abundance n are the SED distributions shown in Fig. 4 (for the 12 most abundant species in the plot). Graphs of SEDs are shown in order from smallest average photosynthetic area (ANDSEP, *Androsace septentrionalis*) to largest (HELQUI, *Helianthella quinquenervis*). Visual inspection of graphs of SEDs for these 12 most abundant species reveals a particular trend: METE overpredicts metabolic rates for species with low average size (size measured in normalized photosynthetic area), does well in approximating the shape and variance of mid-sized species, and underpredicts metabolic rates for species with large average size. This trend holds for all of the 12 most abundant species when ranked by average size of an individual by species, but is not generally upheld when all species are included (see Appendix D). We note a strong effect of abundance, in that this pattern is not upheld for species with 15–20 or fewer individuals (a limit which may be

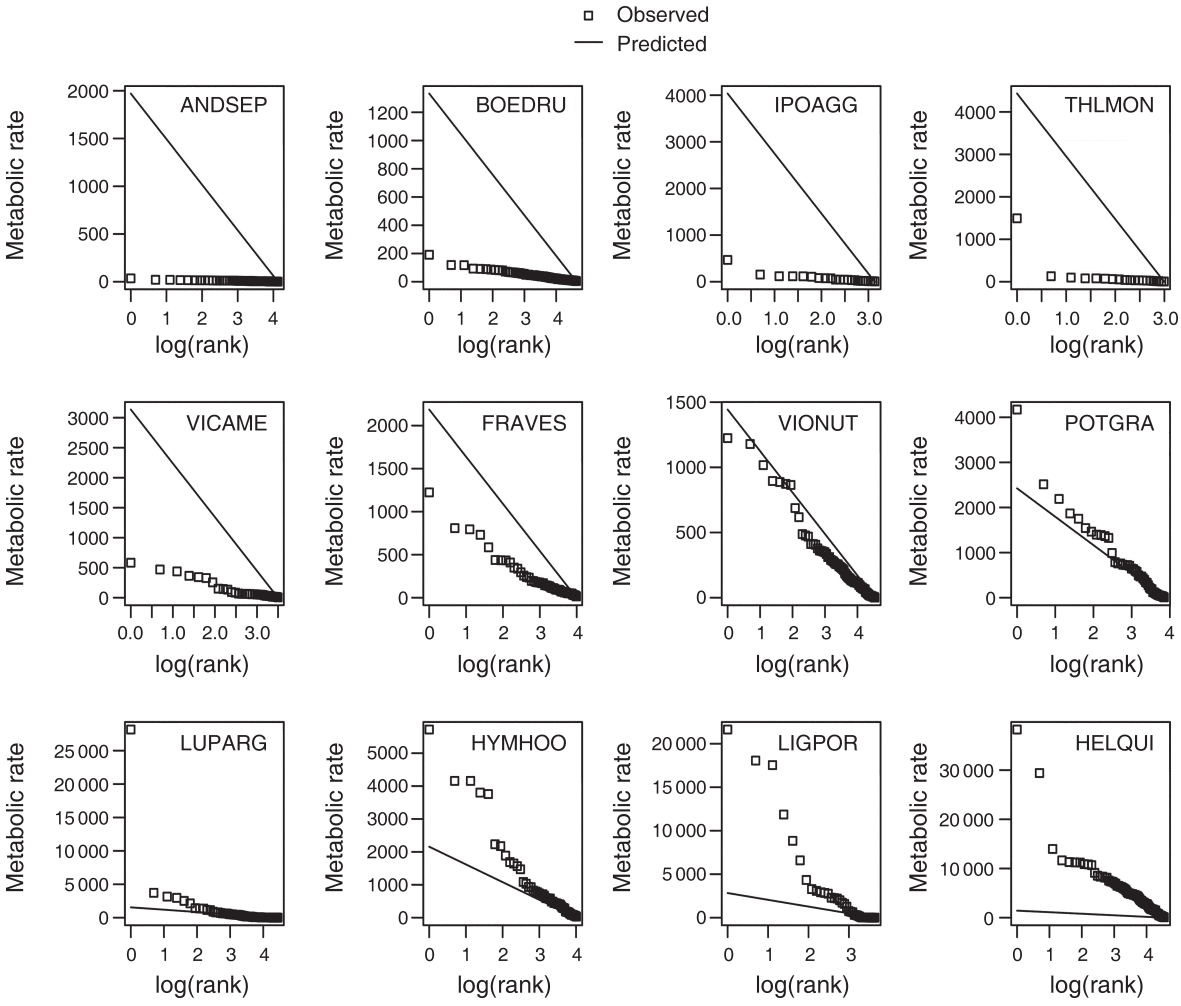

FIG. 4. METE predicted and observed species-level energy distributions (SED) for all individuals of the 12 most abundant species in the subalpine plot. Individuals are ranked from largest to smallest metabolic rate within the species, and graphs are presented in order from smallest to largest average metabolic rate per species. Species codes defined in Table 1.

related to the log-normality of the empirical SAD, see *Discussion*).

This trend in the data is evident when the slopes of the log(observed) vs. log(predicted) values for each species are calculated and then graphed in order from largest average metabolic rate to smallest average metabolic rate (see Fig. 5 and Appendix E: Figs. E1 and E2). Species with individuals that are large on average are more likely to have slopes close to 1, and species that are smaller on average have much larger log(observed) vs. log(predicted) slopes. When log(slopes) are graphed against species ranked by average metabolic rate, a straight line regression is obtained with an R^2 value of 0.71. This regular deviation in slopes of predicted vs. observed data on a log-log scale may reveal a bias in the theoretical prediction of the SEDs that is correlated to the average metabolic rate (or alternately, rank) of each species.

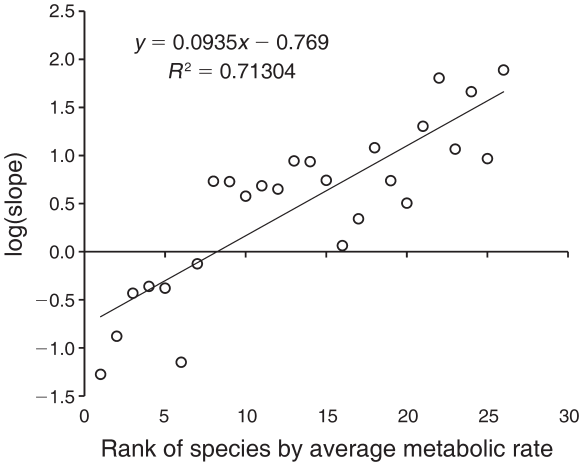

FIG. 5. Slope of predicted vs. observed data for all SEDs with $n \geq 5$ on a log-rank graph. Each point represents one species. A good fit would be characterized by a trend line with slope = 0.



PLATE 1. View of subalpine meadows and Gothic Mountain at the Rocky Mountain Biological Laboratory in Colorado, USA. Photo credit: E. A. Newman.

DISCUSSION

The distributions IED, ASED, and SED

From goodness-of-fit tests, there is mixed evidence that the IED, a community-level metric that predicts the distribution of metabolic rates of all individuals, is successful. Although the IED fails the stringent K-S test, the shape of the predicted distribution is correctly monotonically decreasing with increasingly negative slope. The predicted IED is also constrained to have the same mean and total energy as the empirical data. The IED, therefore, shows promise as a candidate null model for an individual size distribution (ISD)-type prediction, as discussed in White et al. (2007).

In its current mathematical formulation, the SED metric is not flexible enough to capture the range of body sizes in the system we tested. Because the empirical data can be approximated with a decreasing linear fit on log(rank) vs. metabolic rate graphs (see Fig. 4), the exponential form of the SED predictions appears to be an adequate model; however, there is a clear pattern of bias in the slopes of the predicted SEDs related to average body size of a species as described in *Results: Species-level energy distributions*. This suggests that the exponential form of the SED may indeed be an adequate null model, but because the slopes of the predictions are incorrect, it also suggests that the exponent itself could be adjusted to include information about the rank of the average metabolic rate of the species being considered (see Appendix E for further discussion). A modification of the exponent of the SED would give predictions closer to empirical values; however, tests of the SED with more than one data set might better justify a change of the theoretical form.

Problems with the SED are expected to translate to problems with the ASED because the ASED is the predicted distribution of the means of the SEDs. This, by itself, is a large enough effect to cause the ASED to fail; however, we also find that the means of the predicted and observed ASED do not match for unrelated reasons, and the METE prediction, therefore, does not provide a function that is a useful description of this metric. This problem led us to look at a related metric that we call the total species energy distribution (TSED), which has more tractable qualities as a community-level metabolic metric and reproduces results similar to energy equivalence as predicted by Damuth (1987). See Appendix K for a discussion of the failure of the ASED and the properties and predictions of the TSED metric.

Distinguishing the role of disturbance from the failure of theory

Data from the subalpine meadow system show a log-normal trend in the empirical SAD rather than the predicted Fisher log-series curve (Akaike's information criterion [AIC] evidence ratio = 20.09 in favor of

the log-normal), with fewer than predicted singleton species (one rather than five); see Appendix I. A log-normal distribution of cover by species (Bazzaz 1975) or abundances is often observed in systems that have experienced recent ecological perturbations or natural disturbances (Kempton and Taylor 1974, Hill and Hamer 1998; E. A. Newman, M. Wilber, and J. Harte, *unpublished manuscript*; but see Ulrich et al. 2010). During our study year, unusually high early-season temperatures and lower than average snowpack in the previous winter likely had a perturbing effect on the plant community. In surrounding areas, novel plant communities arose in the year of this study as some plants failed to develop after early freezes, others developed according to photoperiod triggers (D. Inouye, *personal communication*), and some plants showed advanced phenology due to higher than average growing-season temperatures and earlier than average snowmelt, a major influence on plant phenology in the region (Dunne et al. 2003).

From this empirical deviation from theory, we could conclude that the values and ratios of the four state variables (A_0, S_0, N_0, and E_0) are not sufficient to describe the dynamics of a real system, such as changes following natural disturbance and other ecological perturbations. It has been suggested elsewhere that evolutionary processes, including diversification and extinction, may influence the shape of empirical macroecological distributions (Hubbell 2001, Harte 2011, Harte and Newman 2014). These explanations, while plausible, would not allow us to distinguish between the role of disturbance in causing theory to fail vs. an inherent flaw with the mathematical construction of theory, so we investigated incorporating the empirical SAD into the METE predictions.

Because of the aforementioned ecological perturbation and the community restructuring effect it may have had, we incorporate the empirical SAD in the elements of the SEDs and ASED that are explicitly dependent on the SAD (see Eq. 4). Predictions of the SEDs and ASED that result from using the empirical SAD and calculating the metrics numerically are presented in Appendix J, with the ASED and example SED shown in Fig. 6a and b. These analyses, while debatably not a direct test of METE's predictions, have allowed us to determine that the log-normality of the empirical SAD does not greatly change the shape of the predicted SEDs and ASED and merely shifts the predictions by some normalization constant. The empirical SAD is, therefore, not the cause of the mismatch between data and theory. We conclude that the problem is likely located within the prediction of the SED because its exponential form appears to be correct except for the predicted slopes and intercepts of the SEDs (see Figs. 4 and 5). We therefore suspect that the predicted exponent of the SED equation is incorrect. This would further explain why the SEDs and ASED jointly fail. In spite of this, the IED remains a largely successful metric because it is free of this particular problem. These results are consistent with an independent study of tree communities (Xiao et al. 2013), suggesting that the observed relationships between the theoretical predictions and empirical data may be general, at least within plants.

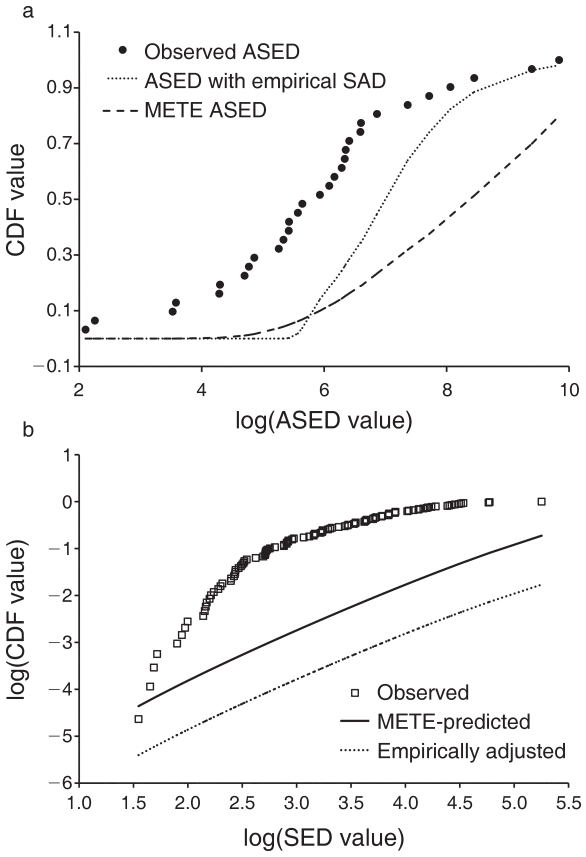

FIG. 6. ASED and example SED showing a comparison of observed values, the METE prediction including the empirical adjustment, and the METE prediction. (a) Cumulative density function (CDF) of the ASED. (b) CDF of the SED for *Boechera stricta*.

CONCLUSIONS

The maximum entropy theory of ecology provides a theoretical basis for estimating various metrics of energetics in biotic communities. Empirical data from a subalpine meadow provide the first explorations of the realism of two of these predictions in a fully censused community. Although we chose an herbaceous plant community because of its tractability and similarity of growth forms within the community, predictions of the community- and species-level metrics considered in this paper should hold generally for any taxon or group of taxa. Future work may reexamine the predicted forms of the metabolic metrics presented here. The IED, the metabolic rate distribution for all individuals in a community, appears successful as a theoretically predicted measure of the

individual energy distribution by linear comparisons of predicted vs. observed data.

Given the poor performance of the METE SAD for this system, we incorporated the empirical, lognormal SAD and found that functional forms of the predicted SEDs are not highly affected by the empirical SAD. By association, METE's metabolic predictions should hold in ecosystems where the shape of the SAD is altered due to natural disturbance or ecological perturbation, succession, or a variety of other ecological factors (Dornelas et al. 2009). Because it appears that the SED is exponential in form, the exponent itself ($\lambda_2 n$) is a likely cause of the highly regular pattern in mismatch between theory and data. The information included in the exponent therefore becomes the target for more theoretical inquiry and empirical testing.

Finally, considering the ASED, we show that the incorporation of the empirical SAD may provide predictions that are closer to empirical data; however, METE fails to predict the correct form of this community-level metric, likely due to the ASED relationship to the SEDs. The predicted ASED also does not necessarily have the same mean as the empirical distribution. A simple conversion of the ASED recovers an energetic-equivalence prediction, the TSED, that is well-normalized and similar to the Damuth Rule. The TSED might be an effective prediction of global-scale metabolic rate distributions, but does not perform well for plot-level metabolic rate distributions.

Acknowledgments

We thank the Rocky Mountain Biological Laboratory for providing permitting, logistical support, and facilities, and Gunnison National Forest for providing field sites. We thank J. Reithel, A. F. Messerman, D. Hembry, J. Kitzes, C. Levy, and A. Rominger for their assistance, and D. Hembry, E. P. White, and X. Xiao for manuscript comments. B. Blonder provided analysis code and much appreciated guidance on methods. Zack Johnson contributed art appearing in this article. Funding was provided by the NSF in the form of the Graduate Research Fellowship Program, Research Experience for Undergraduates program, and grant NSF-EF-1137685.

Literature Cited

Abramoff, M. D., P. J. Magelhaes, and S. J. Ram. 2004. Image processing with ImageJ. Biophotonics International 11:36–42.

Babu, G. J., and E. D. Feigelson. 2006. Astrostatistics: goodness-of-fit and all that! Astronomical Data Analysis Software and Systems XV 351:127–136.

Bazzaz, F. A. 1975. Plant species diversity in old-field successional ecosystems in southern Illinois. Ecology 56: 485–488.

Blonder, B., V. Buzzard, I. Simova, L. Sloat, B. Boyle, R. Lipson, et al. 2012. The leaf-area shrinkage effect can bias paleoclimate and ecology research. American Journal of Botany 99:1756–1763.

Brown, J. H., J. F. Gillooly, A. P. Allen, V. M. Savage, and G. B. West. 2004. Toward a metabolic theory of ecology. Ecology 85:1771–1789.

Clauset, A., D. J. Schwab, and S. Redner. 2009. How many species have mass *M*? American Naturalist 173:256–263.

Cornelissen, J. H. C., et al. 2003. A handbook of protocols for standardised and easy measurement of plant functional traits worldwide. Australian Journal of Botany 5:335–380.

Damuth, J. 1981. Population density and body size in mammals. Nature 290:699–700.

Damuth, J. 1987. Interspecific allometry of population density in mammals and other animals: the independence of body mass and population energy-use. Biological Journal of the Linnean Society 31:193–246.

de Aguiar, M. A. M., M. Baranger, E. M. Baptestini, L. Kaufman, and Y. Bar-Yam. 2009. Global patterns of species and diversity. Nature 460:384–387.

Deng, J.-M., et al. 2008. Trade-offs between the metabolic rate and population density of plants. PLoS ONE 3:e1799.

Dornelas, M., A. C. Moonen, A. E. Magurran, and P. Bàrberi. 2009. Species abundance distributions reveal environmental heterogeneity in modified landscapes. Journal of Applied Ecology 46:666–672.

Dunne, J. A., J. Harte, and K. J. Taylor. 2003. Subalpine meadow flowering phenology responses to climate change: integrating experimental and gradient methods. Ecological Monographs 73:69–86.

Glazier, D. S. 2006. The 3/4-power law is not universal: evolution of isometric, ontogenetic metabolic scaling in pelagic animals. BioScience 56:325–332.

Harte, J. 2011. Maximum entropy and ecology: a theory of abundance, distribution, and energetics. Oxford University Press, Oxford, UK.

Harte, J., J. Kitzes, E. A. Newman, and A. J. Rominger. 2013. Taxon categories and the universal species-area relationship (a comment on Šizling et al., "Beyond geometry and biology: the problem of universality and the species-area relationship"). American Naturalist 181:282–287.

Harte, J., and E. A. Newman. 2014. Maximum information entropy: a foundation for ecological theory. Trends in Ecology and Evolution 29:384–389.

Harte, J., A. Smith, and D. Storch. 2009. Biodiversity scales from plots to biomes with a universal species-area curve. Ecology Letters 12:789–797.

Harte, J., T. Zillio, E. Conlisk, and A. Smith. 2008. Maximum entropy and the state variable approach to macroecology. Ecology 89:2700–2711.

Hill, J. K., and K. C. Hamer. 1998. Using species abundance models as indicators of habitat disturbance in tropical forests. Journal of Applied Ecology 35:458–460.

Hubbell, S. P. 2001. The unified neutral theory of biodiversity and biogeography. Princeton University Press, Princeton, New Jersey, USA.

Jaynes, E. T. 1979. Where do we stand on maximum entropy? Pages 15–118 *in* R. D. Levine and M. Tribus, editors. The maximum entropy formalism. MIT Press, Cambridge, Massachusetts, USA.

Jaynes, E. T. 1982. On the rationale of maximum entropy methods. Proceedings of the IEEE 70:939–952.

Jaynes, E. T. 2003. Probability: the logic of science. Cambridge University Press, Cambridge, UK.

Kempton, R. A., and L. R. Taylor. 1974. Log-series and log-normal parameters as diversity discriminants for the Lepidoptera. Journal of Animal Ecology 381–399.

Makarieva, A. M., V. G. Gorshkov, B.-L. Li, S. L. Chown, P. B. Reich, and V. M. Gavrilov. 2008. Mean mass-specific metabolic rates are strikingly similar across life's major domains: evidence for life's metabolic optimum. Proceedings of the National Academy of Sciences USA 105:16994–16999.

McGill, B. J. 2010. Towards a unification of unified theories of biodiversity. Ecology Letters 13:627–642.

Mori, S., et al. 2010. Mixed-power scaling of whole-plant respiration from seedlings to giant trees. Proceedings of the National Academy of Sciences USA 107:1447–1451.

Muller-Landau, H. C., et al. 2006. Testing metabolic ecology theory for allometric scaling of tree size, growth, and mortality in tropical forests. Ecology Letters 9:575–588.

Niklas, K. J., and B. J. Enquist. 2001. Invariant scaling relationships for interspecific plant biomass production rates and body size. Proceedings of the National Academy of Sciences USA 98:2922–2927.

Reich, P. B., M. G. Tjoelker, J. L. Machado, and J. Oleksyn. 2006. Universal scaling of respiratory metabolism, size and nitrogen in plants. Nature 439:457–461.

Rüger, N., and R. Condit. 2012. Testing metabolic theory with models of tree growth that include light competition. Functional Ecology 26:759–765.

Ulrich, W., M. Ollik, and K. I. Ugland. 2010. A meta-analysis of species–abundance distributions. Oikos 119:1149–1155.

van Rossum, G., and F. L. Drake. 2001. Python Reference Manual. PythonLabs, Virginia, USA. https://docs.python.org/2.0/ref/ref.html

White, E. P., S. K. Ernest, A. J. Kerkhoff, and B. J. Enquist. 2007. Relationships between body size and abundance in Ecology. Trends in Ecology and Evolution 22:323–30.

White, E. P., K. M. Thibault, and X. Xiao. 2012. Characterizing species abundance distributions across taxa and ecosystems using a simple maximum entropy model. Ecology 93:1772–1778.

Xiao, X., D. J. McGlinn, and E. P. White. 2013. A strong test of the Maximum Entropy Theory of Ecology. arXiv preprint arXiv:1308.0731.

Supplemental Material

Appendix A

Measurements and calculations of photosynthetic area (*Ecological Archives* E095-244-A1).

Appendix B

Species-level energy distribution (SED) predictions and observed values for all species with five or more individuals, including comparisons of predicted vs. observed values (*Ecological Archives* E095-244-A2).

Appendix C

Species included in this study ranked by average metabolic rate per species (a normalized measure of photosynthetic area) from largest to smallest (*Ecological Archives* E095-244-A3).

Appendix D

SED predictions and observed values for the 15 most abundant species (*Ecological Archives* E095-244-A4).

Appendix E

Additional analysis of SEDs (*Ecological Archives* E095-244-A5).

Appendix F

The functional form of the average species energy distribution (ASED; ν) as derived from a discrete cumulative distribution function (*Ecological Archives* E095-244-A6).

Appendix G

Kolmogorov-Smirnov goodness-of-fit tests for ASED, individual-level energy distribution (IED), and all SEDs (*Ecological Archives* E095-244-A7).

Appendix H

Additional information on the ASED, including tests of goodness-of-fit (*Ecological Archives* E095-244-A8).

Appendix I

The species-abundance distribution (SAD) of a subalpine plant community (*Ecological Archives* E095-244-A9).

Appendix J

Incorporating the empirical SAD into ASED and SED predictions (*Ecological Archives* E095-244-A10).

Appendix K

Discussion of the normalization of the ASED, and exploration of a related metric, the total species energy distribution (*Ecological Archives* E095-244-A11).

All in-text references underlined in blue are linked to publications on ResearchGate, letting you access and read them immediately.